# The Origin of the Superstructure in $Bi_2Sr_2CaCu_2O_{8+\delta}$ as Revealed by Scanning Tunneling Microscopy

M. D. KIRK, J. NOGAMI, A. A. BASKI, D. B. MITZI, A. KAPITULNIK, T. H. GEBALLE, C. F. QUATE

**Real-space images with atomic resolution of the BiO plane of $Bi_2Sr_2CaCu_2O_{8+\delta}$ were obtained with a scanning tunneling microscope. Single-crystal samples were cleaved and imaged under ultrahigh vacuum conditions at room temperature. The images clearly show the one-dimensional incommensurate superstructure along the *b*-axis that is common to this phase. High-resolution images show the position of the Bi atoms, revealing the structural nature of the superlattice. A missing row of Bi atoms occurs either every nine or ten atomic sites in both ⟨110⟩ directions, accounting for the measured incommensurate periodicity of the superstructure. A model is proposed that includes missing rows of atoms, as well as displacements of the atomic positions along both the *a*- and *c*-axis directions.**

THE CRYSTAL STRUCTURE OF $Bi_2Sr_2CaCu_2O_{8+\delta}$ (2:2:1:2) has been widely studied by several different techniques (*1–7*). A striking feature in all these studies is the appearance of an incommensurate superstructure along the *b*-axis of the material. This report uses the notation of Subramanian *et al.* (*1*), where the crystal structure is described by a pseudo-tetragonal unit cell ($a \sim b \sim 5.4$ Å) and the superstructure extends the unit cell along the *a*-axis. It has been widely reported that this structure is predominantly localized to the BiO planes, yet its exact structure is not known (*3, 8*). Moreover, recent x-ray diffraction data shows that while the largest displacement of atomic positions of the metal atoms occurs in the BiO plane, there is a sizable buckling of all the planes, including the CuO planes (*9*). Therefore, the superstructure is believed to affect the superconductivity of the material (*8, 9*). In this report, we present atomic resolution images of the BiO plane of a (2:2:1:2) single-crystal sample that were made with a scanning tunneling microscope (STM) operating under ultrahigh vacuum (UHV) conditions. The principal features in the images that suggest a cause for the observed incommensurate superstructure are rows of missing atoms running along the *b*-axis (occurring every nine or ten atomic sites along both ⟨110⟩ directions) and displacements of the remaining atoms in both the *a*- and *c*-axis directions.

Single-crystal samples of (2:2:1:2) were prepared by mixing powders of $Bi_2O_3$, $Sr(CO_3)_2$, $CaCO_3$, and CuO starting with an elemental Bi:Sr:Ca:Cu ratio of 2.4:2:1:2. The powders were melted at 950°C, cooled at 0.7°C per hour to 750°C, and then oven-cooled to room temperature. A temperature gradient of approximately 30°C was maintained across the crucibles during cooling. Single-crystal x-ray diffraction studies with a four-circle rotating-anode Huber diffractometer demonstrated the single-crystal character of the $Bi_2Sr_2CaCu_2O_{8+\delta}$ samples. From magnetic measurements, the superconducting transition temperature was determined to be 91 K.

All images were taken under UHV conditions ($< 1 \times 10^{-10}$ torr) using an STM that has been described earlier (*10*). Sample surfaces were prepared by cleaving in situ. All images presented here were taken with electrons tunneling into the sample, voltage biases of 0.15 to 2.0 V, and tunneling currents between 0.2 and 0.5 nA. At this polarity, the STM is sensitive to the unoccupied electronic states of the surface. It was also possible to record images while tunneling out of the sample at voltages up to 1 V; however, the tunneling current was difficult to stabilize with this polarity. A similar dependence on tip bias polarity was noted by Tang *et al.* (*11*). Low energy electron diffraction (LEED) patterns were obtained in the same chamber on all samples after they had been imaged by STM.

In the (2:2:1:2) crystal structure there are two adjacent BiO planes (3.2 Å apart) that are weakly held together (*2, 4*). It is this weak link in the crystal structure that results in a preferential cleavage between the BiO planes. Previous studies on this material, including STM, photoemission, and transmission electron microscopy (TEM), confirm that the cleaved surface is a BiO plane that has a stable structure for several hours in vacuum (*3, 5, 6*). Further, the lamellar nature of the crystal suggests that the surface structure of the BiO plane may be similar to that in the bulk. Figure 1 is a gray scale image (150 Å by 200 Å) of the *z*-piezo displacement taken in constant-current mode at 0.15-V bias and 0.2-nA tunneling current. In the image one can clearly see the atomic structure forming a square lattice of bright dots. Bright regions in an STM image are the result of either a local increase in the density of states or a feature raised from the surface. Density of states calculations by several groups assert that the states at and above the Fermi level of the BiO plane are primarily Bi-derived; therefore, the bright dots in the image are believed to be the Bi atoms (*12–14*). The position of the O atoms cannot be determined from these images. The value measured from the images for the spacing between Bi atoms (4.1 ± 0.3 Å) is consistent with the Bi–Bi length of 3.8 Å reported by several groups (*2, 4*). Running diagonally to the square lattice are rows of depressions that are approximately one or two atomic sites in size. These features appeared as holes at either bias-voltage polarity, suggesting that they are the result of missing atoms rather than substitutional impurities. Further evidence supports this conclusion. The Bi–O bond lengths are too small to accommodate the Sr or Ca atoms (*2, 4*) and Cu substitution would introduce states at the Fermi level that would be visible in the images.

Figure 2, top, is an image of another crystal, prepared and characterized identically, at a slightly higher magnification (100 Å by 60 Å). By superimposing a grid on the image, one can see that the vacancies making up the dark rows are in registry with the adjacent atomic sites. After counting over several regions of various images, it was found that on average one out of every 9.6 ± 0.2 Bi sites (along both ⟨110⟩ directions) was vacant, which agrees well with the incommensurate superstructure period measured using electron diffraction (*3*).

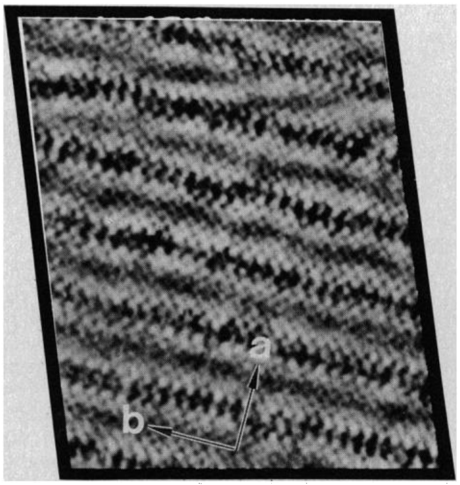

**Fig. 1.** An image (~150 Å by 200 Å) taken at 0.15-V bias and 0.2-nA tunneling current. The square lattice of bright dots indicates the positions of the Bi atoms. The superstructure consists of dark rows running parallel to the *b*-axis and a modulation of atomic heights between these rows.

---

Department of Applied Physics, Stanford University, Stanford, CA 94305.

One can see that the atoms on either side of the missing rows are raised by a buckling of the surface, appearing as the brightest parts in the image. Figure 2, center, is an amplitude trace along the path indicated by the heavy line in Fig. 2, top. In this line scan the buckling displacement appears as a smooth low frequency corrugation with the atomic corrugation superimposed. At each apex of the buckling displacement there is a sharp dip due to a missing atom. Figure 2, top, also shows a slight longitudinal displacement of the atoms running perpendicular to the rows of missing atoms. This longitudinal displacement is visible as an S shape in either the horizontal or vertical rows of bright dots. Figure 2, bottom, demonstrates how the combination of perpendicular S-wave lateral distortions in the lattice is equivalent to a longitudinal displacement modulation running diagonally to the superimposed grid in Fig. 2, top. From these images the amplitude of compression along the *a*-axis is estimated to be 0.5 ± 0.15 Å, a value consistent with a recent x-ray study by Gao *et al.* (0.39 Å) (*9*). In addition, the relative phase between the longitudinal displacements in the *a*-*b* plane and the buckling displacements out of the plane also agrees with the x-ray data. Specifically, the point of maximum upward buckling coincides with the maximum expansion of the Bi–O bond along the *a*-axis.

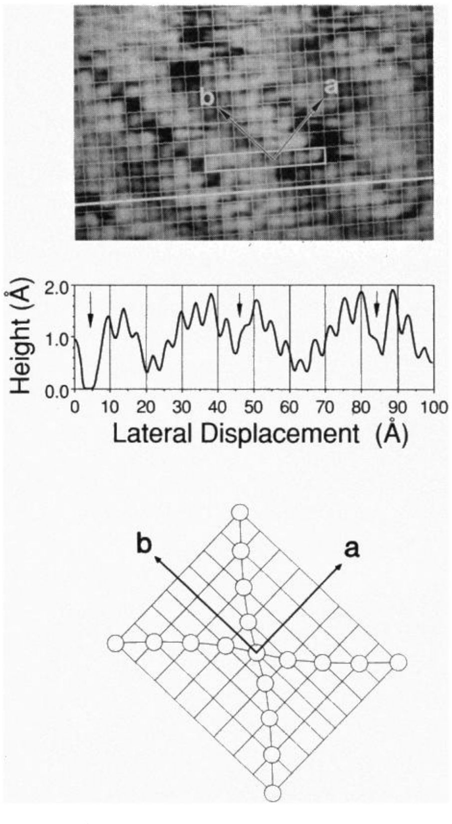

**Fig. 2.** (**Top**) An image (taken at 1.2-V bias) that extends over 100 Å by 60 Å. A grid is superimposed to demonstrate that the vacancies making up the dark rows are in registry with the surrounding atoms. A slight S shape of each Bi row is also apparent, an example of which is shown in the box. (**Center**) An amplitude trace corresponding to the heavy line in the image above. In this line scan the buckling component of the superstructure appears as a low-frequency modulation with the atomic corrugation superimposed. The arrows indicate sites of the missing Bi atoms. (**Bottom**) A diagram that demonstrates that the combination of perpendicular S displacements of the atomic rows reflects a longitudinal compression of the lattice (seen as a change in the size of the grid squares) along the diagonally oriented *a*-axis.

There are two discrepancies between the x-ray study and these STM measurements. The first discrepancy is the magnitude of the out-of-plane buckling displacement. Though the measured buckling amplitude varied with tip bias voltage, it was always within a factor of 3 of the value obtained by Gao *et al.* (*9*). In x-ray studies this amplitude has been seen to increase slightly with decreasing sample thickness, which suggests that surface effects might play a role. However, the magnitude of the discrepancy between the STM and the bulk measurements makes it more likely that the large vertical corrugation amplitude is an artifact of the imaging process, resulting from either an effect of the surface electronic structure, or a mechanical interaction between the tip and surface. The second discrepancy is the suggestion by Gao *et al.* (*9*) that the superstructure is mostly displacive in nature. Although many features of the displacements measured here agree with the earlier work, the presence of Bi vacancies, which can be considered a compositional modulation, is a key feature of this model. Gao *et al.* do suggest that their data could be better fit if the bulk stoichiometry was 10% deficient in Bi and 4% deficient in Sr (*9*). In any event, the agreement between the STM data and the x-ray data of the bulk crystal structure is striking.

Figure 3 is a 600 Å by 600 Å picture that shows the superstructure on a large scale with a periodicity of 26 ± 1.5 Å. This image is similar to those observed by STM in air (*6*). The missing row structure is correlated over large distances; in fact, the superstructure has been observed over thousands of angstroms. LEED patterns taken immediately after imaging also showed the superlattice. The orientation of the *b*-axis from the LEED patterns was always consistent with that inferred from the STM images and the patterns themselves were also consistent with the LEED data reported on identical samples by Lindberg *et al.* (*15*).

It should be noted that the missing row structure was only clearly observed under the best imaging conditions. Other images showed clear atomic corrugation, but the superlattice appeared as a smooth sinusoidal modulation perhaps because of multiple tip tunneling.

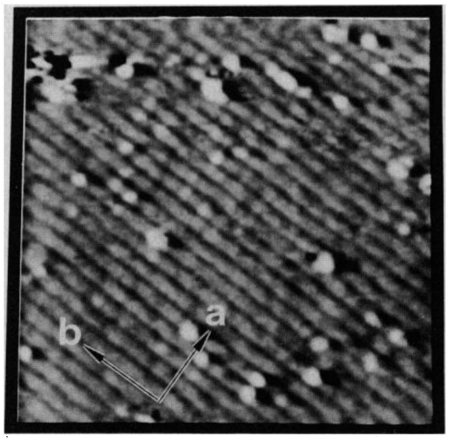

**Fig. 3.** An image (600 Å by 600 Å) taken at 1.5-V bias. A superstructure with a periodicity of 26 Å is seen to extend over large distances. The bright dots are caused by contamination or defects. The wavy character of the lines is caused by the shift from nine to ten atomic sites between missing rows.

Ultimately, the superstructure is caused by a lattice strain arising from a mismatch in the perovskite layers (*2, 8*). The *a* and *b* dimensions of the bulk unit cell are set by the length of the Cu–O bond in the plane. Because the Bi atoms share a common O atom with the CuO plane below and the Cu–O bond is much more rigid, the BiO plane will distort to match the crystal structure imposed by the CuO plane. Because the Bi–O bonds are small, they will expand and buckle to accommodate the CuO plane, but the strain field created will affect the entire crystal structure.

The following model is proposed for the superstructure based on the STM images. Halfway between the missing rows of atoms the Bi–O bond distance is slightly compressed from the average value and is closer to its natural value. This longitudinal compression causes the slight S-shape visible in the images. Stepping along the [100] direction, the Bi–O bond length expands and buckles so as to better match the bond lengths imposed by the CuO plane below. Eventually this stretching of the Bi–O bond is not energetically favorable and the Bi simply skips a site, resulting in a missing row of atoms. If the Bi atom on every ninth or tenth site is missing (an average of every 9.6 sites), then this model will predict the incommensurate superstructure periodicity measured in the bulk.

If the surface structure reflects that of the bulk, then this model leads to a Bi-poor stoichiometry (approximately 10% deficient), yet measurements of these (2:2:1:2) compounds made by other groups conclude that crystals of this type are typically slightly

Bi-rich, and Sr- and Ca-poor (2). Extra Bi atoms may occupy Sr or Ca sites to compensate for the Bi vacancies in the BiO planes. Rutherford backscattering and microprobe analyses of these particular crystals suggested that they were slightly Bi-rich, but the spread in the data makes such measurements inconclusive.

In conclusion, an STM operating in UHV conditions has been used to resolve the atomic structure of the BiO surface plane of single-crystal $Bi_2Sr_2CaCu_2O_{8+\delta}$. Missing rows of Bi atoms and a displacive modulation of the Bi atoms both parallel and perpendicular to the *a*-*b* plane are responsible for the superstructure seen in this compound. The missing rows occur on every ninth or tenth lattice site, yielding an average spacing that agrees with the incommensurate perodicity seen in TEM and x-ray data of the bulk crystal structure. The lateral displacive modulation measured by STM has the same amplitude and phase (relative to the phase of the vertical buckling modulation) as those seen by x-ray measurements of the bulk. Thus, the structure of the surface BiO plane corresponds to that of the bulk BiO planes. Because the double BiO layers in the bulk are weakly held together, the surface reconstruction of the BiO plane is expected to be small. X-ray data has shown that the Cu atoms in the (2:2:1:2) crystal are buckled, perturbing the electronic states of the CuO plane. Other superstructures have been recently measured in the related Tl containing compounds (16). Therefore, the superstructure studied in the (2:2:1:2) compound may not just be an oddity of this complicated crystal structure. In fact, such superlattice behavior may critically affect the superconducting properties of this class of cuprate superconductors.

### REFERENCES AND NOTES

1. M. A. Subramanian *et al.*, *Science* **239**, 1015 (1988).
2. S. A. Sunshine *et al.*, *Phys. Rev. B* **38**, 893 (1988).
3. T. M. Shaw *et al.*, *ibid.* **37**, 9856 (1988).
4. J. M. Tarascon *et al.*, *ibid.*, p. 9382.
5. P. A. P. Lindberg *et al.*, in preparation.
6. M. D. Kirk *et al.*, *Appl. Phys. Lett.* **52**, 2071 (1988).
7. The first atomic resolution images in air on (2:2:1:2) were taken by Virgil Elings (Digital Instruments) and were presented at the Third International STM Conference, Royal Microscopical Society, Oxford, England, 4 to 8 July 1988.
8. H. W. Zandbergen, P. Groen, G. Van Tendeloo, J. Van Landuyt, S. Amelinckx, *Solid State Commun.* **66**, 397 (1988).
9. Y. Gao, P. Lee, P. Coppens, M. A. Subramanian, A. W. Sleight, *Science* **241**, 954 (1988).
10. S. Park and C. F. Quate, *Rev. Sci. Instrum.* **58**, 2010 (1987).
11. S. L. Tang, R. V. Kasowski, M. A. Subramanian, W. Y. Hsu, *Physica C* **156**, 177 (1988).
12. M. S. Hybertsen and L. F. Mattheiss, *Phys. Rev. Lett.* **60**, 1661 (1988).
13. H. Krakauer and W. E. Pickett, *ibid.*, p. 1665.
14. F. Herman, R. V. Kasowski, W. Y. Hsu, *Physica C* **153–155**, 629 (1988).
15. P. A. P. Lindberg *et al.*, *Appl. Phys. Lett.*, in press.
16. R. Beyers *et al.*, *ibid.* **53**, 432 (1988).
17. The authors thank A. Marshall, R. Barton, and W. Harrison for useful discussions. L. LaComb assisted with image processing software. Three of the authors would like to acknowledge support received through AT&T Ph.D. Fellowships (A.A.B. and D.B.M.) and Alfred P. Sloan and P.Y.I. Fellowships (A.K.). This work was supported by the Defense Advanced Research Projects Agency, the Office of Naval Research, and by the National Science Foundation Materials Research Laboratory Program through the Center for Materials Research at Stanford University.

27 October 1988; accepted 18 November 1988

# Gravitational Separation of Gases and Isotopes in Polar Ice Caps

H. Craig, Y. Horibe,[*] T. Sowers[†]

**Atmospheric gases trapped in polar ice at the firn to ice transition layer are enriched in heavy isotopes (nitrogen-15 and oxygen-18) and in heavy gases ($O_2/N_2$ and $Ar/N_2$ ratios) relative to the free atmosphere. The maximum enrichments observed follow patterns predicted for gravitational equilibrium at the base of the firn layer, as calculated from the depth to the transition layer and the temperature in the firn. Gas ratios exhibit both positive and negative enrichments relative to air: the negative enrichments of heavy gases are consistent with observed artifacts of vacuum stripping of gases from fractured ice and with the relative values of molecular diameters that govern capillary transport. These two models for isotopic and elemental fractionation provide a basis for understanding the initial enrichments of carbon-13 and oxygen-18 in trapped $CO_2$, $CH_4$, and $O_2$ in ice cores, which must be known in order to decipher ancient atmospheric isotopic ratios.**

ISOTOPIC RATIOS OF ATMOSPHERIC gases trapped in polar ice cores provide important data for understanding the atmospheric history of $O_2$ (1–3), $CO_2$ (4), and $CH_4$ (5), and the past variations in sources and sinks of these gases. Thus it is essential that fractionation mechanisms in polar firn layers that may affect the composition (isotopic and chemical) of gases before trapping in nascent ice beneath the firn be identified and understood. Horibe *et al.* (1) originally reported that $O_2$ trapped in 2000-year-old ice from Camp Century, Greenland, has an $^{18}O/^{16}O$ enrichment given by $\delta(^{18}O) = 0.61$ per mil versus present-day atmospheric $O_2$ (6). Bender *et al.* (2) reported essentially zero $^{18}O$ enrichments in $O_2$ in Holocene ice from the Antarctic D-10 and Dome C cores, with, however, significant enrichments in $O_2$ in Pleistocene ice in these cores, similar to those observed in older Greenland ice (1). These data therefore indicated that fractionation effects during accumulation of firn, possibly occurring only in Greenland ice, might affect the isotopic records of $O_2$ and other gases in ice cores.

In this report we show that $^{15}N$ and $^{18}O$ enrichments are present in $N_2$ and $O_2$ in Recent ice from Greenland Dye 3 ice core. One of us (3) has observed similar enrichments in Greenland and Antarctic ice, together with variations in major gas composition. We propose that the major fractionation process affecting these gases and isotopes is gravitational separation in the firn layer above the ice. Other effects on gas chemistry appear to reflect differential gas losses in accordance with experimental observations and expected capillary conduc-

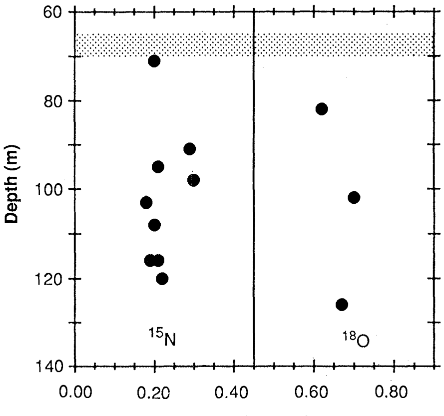

**Fig. 1.** Measurements of $\delta(^{15}N)$ and $\delta(^{18}O)$ relative to air in trapped $N_2$ and $O_2$ in the Dye 3 Greenland ice core, versus depth. Experimental precision is ~±0.05 per mil for each isotope (6). The firn to ice transition (stippled region) is at 65 to 70 m (8).

H. Craig and Y. Horibe, Isotope Laboratory, Scripps Institution of Oceanography, University of California at San Diego, La Jolla, CA 92093.
T. Sowers, University of Rhode Island, Graduate School of Oceanography, Narragansett, RI 02882.

---

[*] Present address: School of Marine Science, Tokai University, Shizuoka, Japan 424.
[†] Present address: Laboratoire Glaciologie et Geophysique de l'Environnement, BP 96, 39402 Saint Martin d'Heres, Cedex, France.